CFD ANALYSIS OF FLOW AND CONCENTRATION FIELDS AROUND A BUILDING WITH A ROOF STACK

Y. Tominaga[1†], and T. Stathopoulos[2]

[1]*Department of Architecture and Building Engineering, Niigata Institute of Technology, 1719 Fujihashi, Kashiwazaki, Niigata, Japan*
[2]*Centre for Building Studies, Department of Building, Civil and Environmental Engineering, Concordia University*

ABSTRACT

The prediction of plume dispersion near buildings is very important for the design of exhaust stacks and air intakes in order to avoid adverse air quality impacts. However, it is difficult to predict pollutant dispersion with certain accuracy due to the complex interaction between atmospheric flow and flow around buildings. Although Computational Fluid Dynamics (CFD) techniques are widely utilized to study the wind field and pollutant transport near and around buildings through rapid development in computer hardware and numerical modeling, the prediction accuracy of the quantitative values for these phenomena is not so clear.

In this paper, the prediction accuracy of the flow and dispersion around a cubic building with a flush stack located on the roof were examined using various k-ε models. Numerical results were compared with the wind tunnel data. The pollutant distributions were well predicted with the modified k-ε models. It was confirmed that the predicted concentrations by all CFD models were less diffusive than those of the experiment and the results were largely dependent on the value of turbulent Schmidt number.

KEYWORDS

CFD, Dispersion, Building, Turbulence model, Stack

INTRODUCTION

The prediction of plume dispersion near buildings is very important for the design of exhaust stacks and air intakes in order to avoid adverse air quality impacts. The methods often used to predict pollutant dispersion around a building are Gaussian model and empirical formulae, such as ASHRAE models, which are based on the concentration measurements obtained in the wind or water tunnel simulation (Wilson, 1982, 1983). However, results of these methods provide little information for dispersion analysis, such as an expected minimum dilution factor or a recommended stack height, and also have difficulty to be applied to more complex building geometries. On the other hand, CFD techniques can provide flow and dispersion properties around buildings with complex geometric shapes at every point simultaneously. Although there are several studies regarding CFD prediction for dispersion around buildings (Li and Stathopoulos, 1997 ; Meroney et al., 1999), the prediction accuracy of the quantitative values for these phenomena has been questioned.

The relative performance of various turbulence models for flowfield around a building has been studied in several papers (Murakami et al., 1993 ; Mochida et al., 2002), but that for the dispersion problem has not been clarified. Furthermore, the turbulent Schmidt number, Sc_t, which is defined as the ratio of eddy viscosity for momentum to the diffusivity for mass, is necessary to solve the transport mass equation in the CFD prediction of dispersion with RANS models. Several experimental studies suggest that the optimum value of Sc_t varies from 0.3 to 1.0 according to the flow characteristics

† Corresponding Author:
E-mail address: tominaga@abe.niit.ac.jp

(Koeltzsch et al, 2000 ; Flesch, 2002). Therefore, it is difficult to determine a optimum value for Sc_t applied to dispersion in complex flowfield around buildings.

The purpose of this study is to investigate the influence of turbulence models and the value of Sc_t in the prediction of dispersion around an isolated building with a roof stack.

COMPUTATIONAL DETAILS

Flow field

The flow field selected as a test case was the dispersion around a cubic building with a flush stack at the rooftop placed within the neutral surface boundary-layer. Firstly, the wind tunnel measurements of velocity around a cubic model without stack emission were used by the authors for validation of the prediction accuracy of velocity field by CFD (Flow I). In this experiment, wind velocity was measured by a split fibre probe, which can discern three-dimensional components of velocity vector. The Reynolds number based on H_b (building height) and U_b (inflow velocity at $z=H_b$) was 6.4x104. Next, the wind tunnel measurements by Li and Meroney (1983) were used for the comparison in the concentration field with stack emission (Flow II). Three vent locations, i.e. upwind roof, central roof and downwind roof, were considered in the computations comparing with the experiment. The Reynolds number based on H_b and U_b was $1.1x10^4$. Another experimental result with the central vent release for the same configuration by Saathoff et al. (1995) was also compared for reference.

Boundary conditions

The computational domain and boundary conditions, which were commonly used for both Flow I and II, are summarized in Fig. 1. This domain was discretized into 86(x)×76(y)×46(z) grids. The minimum grid width is $0.0045H_b$ (H_b is the building height). The vertical distributions of the quantities at the inflow boundaries were set based on each experiment. The power law exponents are 0.21 for Flow I and 0.19 for Flow II (Li and Meroney, 1983). The horizontal homogeneities of the turbulent boundary layer with the present boundary conditions in two cases were examined by the computation using an empty domain (Blocken et al., 2006).

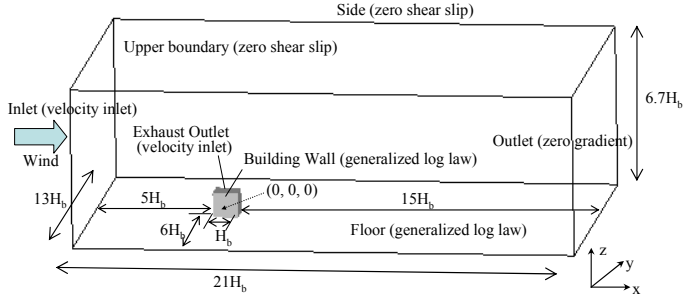

Fig. 1 Computational domain and boundary conditions

Numerical method

Four types of turbulence models, i.e., the standard k-ε model (hereafter SKE), the RNG k-ε model (Yakhot et al., 1992 ; hereafter RNG), the modified k-ε model proposed by Durbin (1996) (hereafter DBN) and the Realizable k-ε model (Shih et al., 1995 ; hereafter RLZ) were compared in this study. The expression of eddy viscosity vt and the transport equation of ε for each model are summarized in Table 1. Furthermore, three different values (0.3, 0.7 and 1.0) were used for the turbulent Schmidt number, Sc_t, in selected cases in order to examine its effect on the concentration distribution. Sc_t is needed to estimate the turbulent scalar flux $-\langle u_i'c' \rangle$ assuming the gradient diffusion hypothesis by

$$-\langle u_i'c'\rangle = \frac{\nu_t}{Sc_t}\frac{\partial \langle c\rangle}{\partial x_i} \qquad (20)$$

where, <c> : averaged concentration, c': fluctuating concentration

The QUICK scheme was used for discretizing momentum and concentration equations. The numerical integrations were conducted following the HSMAC method (simultaneous iteration method for pressure and velocity).

Table 1 Model Equations

	Expression of eddy viscosity ν_t	Transport equation of ε
Standard k-ε (SKE)	$\nu_t = C_\mu k\frac{k}{\varepsilon}$ (1), C_μ=0.09	$\frac{\partial\varepsilon}{\partial t}+\langle u_j\rangle\frac{\partial\varepsilon}{\partial x_j}=\frac{\partial}{\partial x_j}\left(\frac{\nu_t}{\sigma_\varepsilon}\frac{\partial\varepsilon}{\partial x_j}\right)+\frac{\varepsilon}{k}\left(C_{\varepsilon1}P_k-C_{\varepsilon2}\varepsilon\right)$ (2) $C_{\varepsilon1}$=1.44, $C_{\varepsilon2}$=1.92, σ_ε=1.3
RNG k-ε (RNG)	$\nu_t = C_\mu k\frac{k}{\varepsilon}$ (1), C_μ=0.085	$\frac{\partial\varepsilon}{\partial t}+\langle u_j\rangle\frac{\partial\varepsilon}{\partial x_j}=\frac{\partial}{\partial x_j}\left(\frac{\nu_t}{\sigma_\varepsilon}\frac{\partial\varepsilon}{\partial x_j}\right)+\frac{\varepsilon}{k}\left(C^*_{\varepsilon1}P_k-C_{\varepsilon2}\varepsilon\right)$ (3) $C^*_{\varepsilon1}=1.42-\frac{\eta(1-\eta/4.38)}{1+0.012\eta^3}$ (4), $\eta=\frac{k}{\varepsilon}S$ (5) $S=\sqrt{2S_{ij}S_{ij}}$ (6), $S_{ij}=\frac{1}{2}\left(\frac{\partial\langle u_i\rangle}{\partial x_j}+\frac{\partial\langle u_j\rangle}{\partial x_i}\right)$ (7) $C_{\varepsilon2}$=1.68, σ_ε=0.719
Durbin k-ε (DBN)	$\nu_t = C_\mu kT$ (8), C_μ=0.09 $T=\min\left(\frac{k}{\varepsilon},\frac{1}{C_\mu\sqrt{6}S}\right)$ (9)	$\frac{\partial\varepsilon}{\partial t}+\langle u_j\rangle\frac{\partial\varepsilon}{\partial x_j}=\frac{\partial}{\partial x_j}\left(\frac{\nu_t}{\sigma_\varepsilon}\frac{\partial\varepsilon}{\partial x_j}\right)+\frac{\varepsilon}{k}\left(C_{\varepsilon1}P_k-C_{\varepsilon2}\varepsilon\right)$ (2) $C_{\varepsilon1}$=1.44, $C_{\varepsilon2}$=1.92, σ_ε=1.3
Realizable k-ε (RLZ)	$\nu_t = C_\mu k\frac{k}{\varepsilon}$ (1), $C_\mu=\frac{1}{4.04+A_S kU^*/\varepsilon}$ (10) $U^*=\sqrt{S_{ij}S_{ij}+\tilde{\Omega}_{ij}\tilde{\Omega}_{ij}}$ (11) $\tilde{\Omega}_{ij}=\Omega_{ij}-2\varepsilon_{ijk}\omega_k$ (12) $\Omega_{ij}=\frac{1}{2}\left(\frac{\partial\langle u_i\rangle}{\partial x_j}-\frac{\partial\langle u_j\rangle}{\partial x_i}\right)$ (13) $A_S=\sqrt{6}\cos\phi$ (14), $\phi=\frac{1}{3}\arccos(\sqrt{6}W)$ (15) $W=\frac{S_{ij}S_{jk}S_{ki}}{\tilde{S}^3}$ (16), $\tilde{S}=\sqrt{S_{ij}S_{ij}}$ (17)	$\frac{\partial\varepsilon}{\partial t}+\langle u_j\rangle\frac{\partial\varepsilon}{\partial x_j}=\frac{\partial}{\partial x_j}\left(\frac{\nu_t}{\sigma_\varepsilon}\frac{\partial\varepsilon}{\partial x_j}\right)+C_1S\varepsilon-C_2\frac{\varepsilon^2}{k+\sqrt{\nu\varepsilon}}$ (18) $C_1=\max\left[0.43,\frac{\eta}{\eta+5}\right]$ (19) C_2=1.9, σ_ε=1.2

RESULTS AND DISCUSSION

Comparison of flow field with various turbulence models

For the four types of turbulence model mentioned in section 2.3, a comparison of the flow around a cube without stack emission (Flow I) is carried out. Fig. 2 shows profiles of streamwise velocities on the roof and behind the cube at the centerline obtained by the four CFD cases and the experiment in the present study. The results obtained by all turbulence models correspond generally well with those of the experiment. However, in the result of the SKE, the reverse flow at x/H_b=-0.25 and 0 on the roof, which was observed in the experiment, was not reproduced as pointed out previously (Murakami, 1993 ;

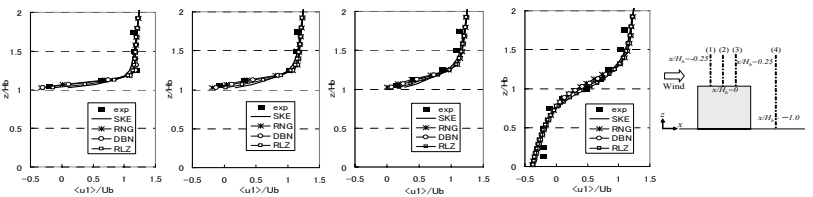

(1) x/H_b=-0.25 (2) x/H_b=0 (3) x/H_b=0.25 (4) x/H_b=1.0

Fig. 2 Comparison of the vertical distribution of streamwise velocity on the roof and behind the cube at centerline

Mochida et al., 2002). On the other hand, the reverse flows on the roof appear in the results of the revised k-ε models, although the results of RLZ under-predict the reverse flow size in comparison with the other two cases (RNG, DBN) and the experiment. In fact, RNG results show the best agreement with the experiment.

Comparison of concentration field with various turbulence models

Fig. 3 shows comparison of the contours of the dimensionless concentration, K, on the roof surface obtained with the present CFD and two experiments (Li and Meroney, 1983 ; Saathoff et al., 1995). In this study, dimensionless concentration K was defined as:

$$K = \frac{< c > H_b^2 U_b}{Q_e} \qquad (21)$$

where Qe is the plume flow rate.

The difference between the two experiments was mainly attributed to the difference of sampling positions for concentration and the interpolation scheme used to obtain the contours (Saathoff et al., 1995).

For this comparison, the turbulent Schmidt number, Sc_t, was set at 0.7 for each case. A significant characteristic of the plume dispersion around an isolated cubic building is that the maxi-mum concentration on the roof occurs upwind of the stack. Clearly, the results from the revised k-ε models (RNG, DBN, RLZ) show better agreement with the wind tunnel experiment than that of SKE. This difference was caused by the well-reproduced reverse flow on the roof in the revised models, which is not observed in SKE as already discussed in section 3.1. The results obtained by RLZ are a little more diffusive in lateral direction than those of the other revised k-ε models.

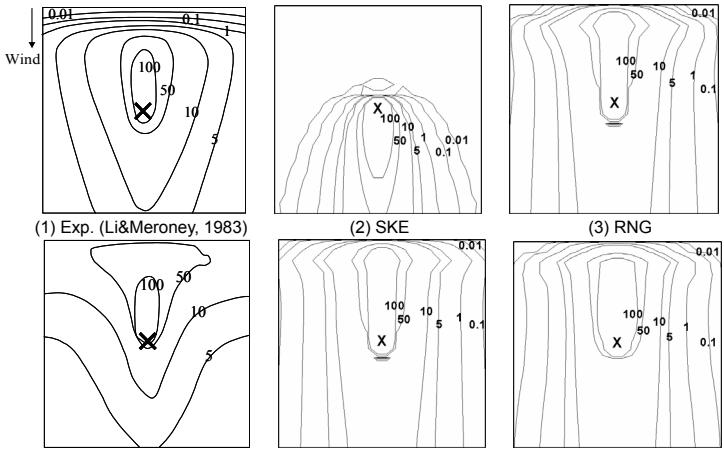

(1) Exp. (Li&Meroney, 1983) (2) SKE (3) RNG

(4) Exp. (Saathoff et al., 1995) (5) DBN (6) RLZ

Fig. 3 Contours of dimensionless concentration K on the roof surface obtained by the experiments and CFD (Central roof vent release)

The distribution of K on centerline of the roof and leeward wall is shown in Fig. 4. The SKE fails to represent the concentration upwind of the stack, while it overestimates the concentration downwind of the stack in comparison with the experiments and the revised models. However, on the back wall, similar distributions of K are predicted by all models. The difference among the revised models compared is not so large in streamwise direction. The computed concentrations behind the cube in all CFD cases are over-predicted in comparison with the experiment. This tendency can be attributed to the over-prediction of the reverse flow behind the cube as shown in Fig. 2(4). Fig. 4(2) shows K distributions on the roof and side wall along the lateral direction. On the side wall, all CFD results

generally under-predict the concentration measured by the experiment, i.e., the diffusion in lateral direction is still underestimated. However, in the area around the edge, the result of RNG shows larger concentration than other models, and it is closer to the experiment. In general, RNG results are the best and SKE results are the worst in terms of reproducing the concentration of exhaust on the roof and the walls of the building.

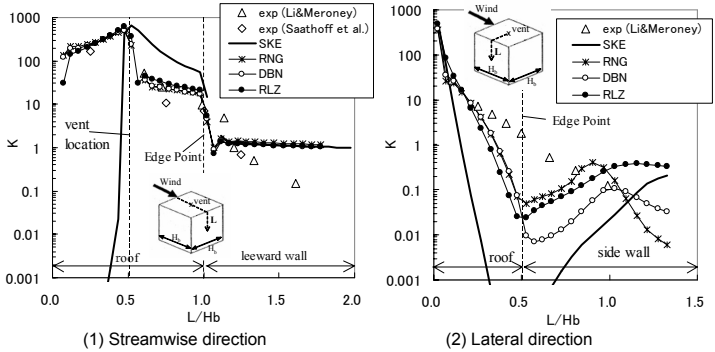

(1) Streamwise direction (2) Lateral direction

Fig. 4 Distribution of dimensionless concentration K on centerline of the roof and leeward wall (Central roof vent release)

Different stack location

The results applying two turbulence models (SKE and RNG) to the experimental cases with the upwind and downwind stack locations respectively are presented in Figs. 5 and 6, in terms of concentration contours K on the roof surface. In the case with upwind release, the difference between the result from SKE and that from RNG was relatively small in comparison to the cases with other stack locations. This is because most of the contaminant was advected by the strong separated flow in streamwise direction. On the other hand, in the case of downwind release, the result obtained by SKE, which does not spread toward upward direction, is completely different from that of the experiment, but the predicted values from RNG correspond well with those from the experiment. These results suggest the possibility that the evaluation of the prediction accuracy for turbulence models on the concentration may change according to the relationship between the stack location and general flow pattern.

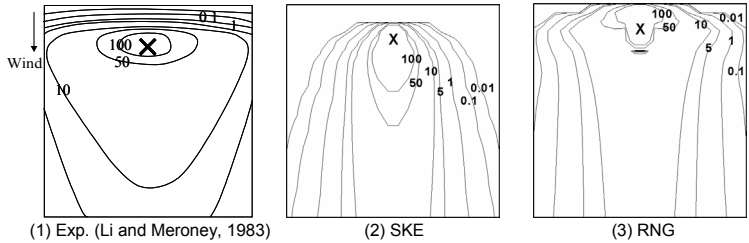

(1) Exp. (Li and Meroney, 1983) (2) SKE (3) RNG

Fig. 6. Contours of dimensionless concentration K on the roof surface obtained by the experiments and CFD (Upwind roof vent release)

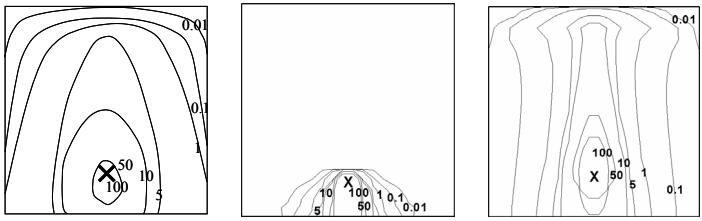

(1) Exp (Li and Meroney, 1983) (2) SKE (3) RNG

Fig. 7. Contours of dimensionless concentration K on the roof surface obtained by the experiments and CFD (Downwind roof vent release)

Influence of turbulent Schmidt number

In this section, the results of RNG using various Sc_t values are shown. Fig. 7 indicates the influence of Sc_t on the contours of K on the roof. The results using Sc_t = 0.3 increase the lateral spread of the plume in comparison with those using Sc_t = 0.7 and 1.0. The difference between Sc_t = 0.7 and 1.0 is very small. Fig. 8 shows K distributions of the roof and leeward wall along the streamwise and lateral directions. At leeward wall, the result with Sc_t = 0.3 also shows smaller value of concentration, which is closer to that from experiment than the results with Sc_t = 0.7 and 1.0. However, the result with Sc_t =0.3 becomes a little more problematic at the side wall. The concentrations on the side wall obtained by Sc_t =0.3 are lower than those from the experiment and the cases with other Sc_t values. This underestimation is due to the decrease of mass transport to side wall from the area behind the cube. Fig. 9 indicates the distribution of turbulent scalar flux in lateral direction adjacent to the stack obtained by CFD with various Sc_t values. These scalar fluxes computed by eqn. (20) have a large peak just beside the stack in all cases. The results with Sc_t =0.3 show maximum values corresponding to the most diffusive distribution of concentration in this case. Consequently, these results agree better with the experiment than those using Sc_t = 0.7 and 1.0.

It should be noted here that it is likely that the underestimation of turbulent diffusion is compensated by the small Sc_t in this case. This is caused by two facts, namely, that the usual RANS computation cannot reproduce unsteady motion such as vortex shedding around a bluff body; and that the gradient diffusion hypothesis to estimate the turbulent mass flux is not valid for such complex flow fields.

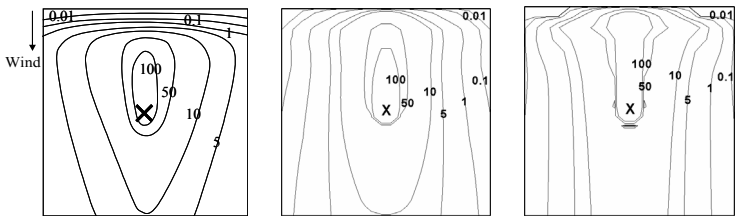

(1) Exp. (Li and Meroney, 1983) (2) RNG with Sc_t = 0.3 (3) RNG with Sc_t = 1.0

Fig. 7. Contours of dimensionless concentration K on the roof surface obtained by the experiment and CFD with various Sc_t numbers (Central roof vent release)

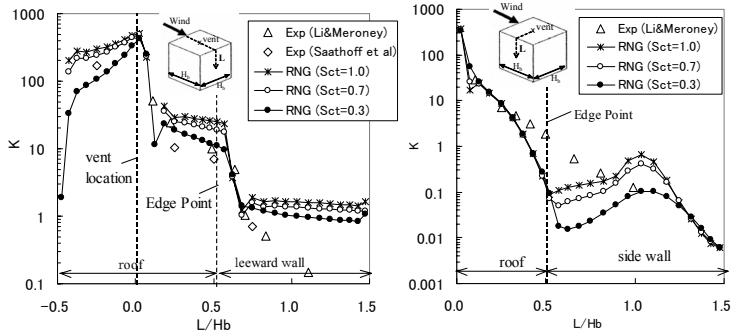

(1) Streamwise direction (2) Lateral direction

Fig. 8. Distribution of dimensionless concentration K on centerline of the roof and leeward wall with various Sc_t numbers (Central roof vent release)

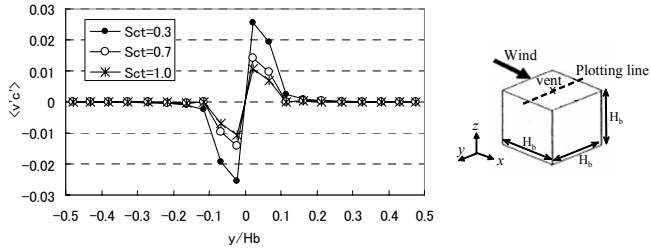

Fig. 9. Distribution of turbulent scalar flux in lateral direction $< v'c' >$ adjacent to the stack with various Sc_t numbers (Central roof vent release)

CONCLUSIONS

The performance of four types of turbulence models was examined for flow and concentration fields around a cube with stack emission in the surface boundary layer. The SKE model provides inadequate results for concentration field, because the basic flow structure such as the reverse flow on the roof can not be reproduced with this model. However, the revised k-ε models considered provide concentrations in better agreement with the experimental data. It is also confirmed that the prediction accuracy of the velocity field strongly affects that of the concentration field. The general agreement with the experiment in the RNG case was the best among the turbulence models tested. For RNG cases with various turbulent Schmidt numbers, Sc_t, the results using Sc_t = 0.3 gave better agreement with the wind tunnel data than those using Sc_t = 0.7 and 1.0.

REFERENCES

1. ASHRAE Applications Handbook, 2003, Chapter 44 Building Air Intake and Exhaust Design.
2. Blocken, B., Stathopoulos, T., Carmeliet, J., 2007, CFD simulation of the atmospheric boundary layer : wall function problems, Atmospheric Environment 41, 238–252.
3. Durbin, P.A., 1996, On the k-εstagnation point anomaly, Int. J. Heat and Fluid Flow 17, 89-90.
4. Flesch, T. K., 2002. Turbulent Schmidt number from a tracer experiment, Agricultural and Forest Meteorology 111, 299-307.
5. Koeltzsch, K., 2000, The height dependence of the turbulent Schmidt number within the boundary layer, Atmos-pheric Environment 34, 1147-1151.

6. Li, W. & Meroney, R. N., 1983, Gas dispersion near a cubical model building, Part I, Mean concentration measure-ments, J. Wind Engrg, & Ind. Aerodyn. 12, 15-33.
7. Li, Y. and Stathopoulos, T., 1997, Numerical evaluation of wind-induced dispersion of pollutants around a building, Journal of Wind Engineering and Industrial Aerodynamics 67-68, 757-766.
8. Meroney, R. N., Leitl, B.M., Rafailidis, S. & Schatzmann, M., 1999, Wind tunnel and numerical modeling of flow and dispersion about several building shapes, Journal of Wind Engineering and Industrial Aerodynamics 81, 333-345.
9. Murakami, S., 1993, Comparison of various turbulence models applied to a bluff body, Journal of Wind Engineering and Industrial Aerodynamics 46-47, 21-36.
10. Mochida, A., Tominaga, Y., Murakami, S., Yoshie, R.,Ishihara, T. and Ooka, R., 2002, Comparison of various k-εmodel and DSM applied to flow around a high-rise building - report on AIJ cooperative project for CFD prediction of wind environment, Wind & Structures 5, No.2-4, 227-244.
11. Saathoff, P. J., Stathopoulos, T. and Dobrescu, M., 1995, Effects of model scale in estimating pollutant dispersion near buildings, Journal of Wind Engineering and Industrial Aerodynamics 54-55, 549-559.
12. Shih, T.H., Liou, W. W., Shabbir, A., Yang, Z. and Zhu, J., 1995, A new k-ε eddy viscosity model for high Reynolds number turbulent flows, Computers and Fluids 24, No.3, 227-238.
13. Wang, X., Stathopoulos, T. & Saathoff, P., 2006, Numerical evaluation of dispersion of pollutants in the building environment: comparisons with models and experiments, The Fourth International Symposium on Computational Wind Engineering, Yokohama, Japan, 805-808.
14. Wilson, D.J. 1977. Dilution of exhaust gases from building surface vents, Trans. Am. Soc. Heating Refrig. Eng., 83, 168-176.
15. Wilson, D.J. 1982. Critical wind speeds for maximum exhaust gas reentry from flush vents at roof level intakes. ASHRAE Transactions 88(1), 503-13.
16. Wilson, D. J. 1983. A Design Procedure for Estimating Air Intake Contamination from Nearby Exhaust Vents, ASHRAE Transactions 89(2), 136-152.
17. Yakhot, V., Orszag, S. A., Thangam, S., Gatski, T. B. and Speziale, C. G., 1992, Development of turbulence models for shear flows by a double expansion technique, Phys. Fluids A 4, 1510-1520.